ELSEVIER

Ecological Modelling 133 (0000) 209–223

ECOLOGICAL MODELLING

www.elsevier.com/locate/ecolmodel

A cellular automaton model for the effects of population movement and vaccination on epidemic propagation

G. Ch. Sirakoulis, I. Karafyllidis*, A. Thanailakis

Laboratory of Electrical and Electronic Materials Technology, Department of Electrical and Computer Engineering, Democritus University of Thrace, GR-671 00 Xanthi, Greece

Received 29 October 1999; received in revised form 17 March 2000; accepted 12 April 2000

Abstract

A cellular automaton model for the effects of population movement and vaccination on epidemic propagation is presented. Each cellular automaton cell represents a part of the total population that may be found in one of three states: infected, immunized and susceptible. As parts of the population move randomly in the cellular automaton lattice, the disease spreads. We study the effect of two population movement parameters on the epidemic propagation: the distance of movement and the percentage of the population that moves. Furthermore, the model is extended to include the effect of the vaccination of some parts of the population on epidemic propagation. The model establishes the acceleration of the epidemic propagation because of the increment, of the percentage of the moving population, or of the maximum distance of population movement. On the contrary, the effect of population vaccination reduces the epidemic propagation. The proposed model can serve as a basis for the development of algorithms to simulate real epidemics based on real data.

Keywords: Cellular automata; Epidemics; Modelling; Population dynamics; Vaccination

1. Introduction

Throughout the 20th century, the formal analogies between the mathematical models in population dynamics and certain models of different physical or chemical processes have been a source of inspiration for biologists, physicists and engineers. Epidemics constitute a very important topic in biology, bioengineering, medicine, mathematics and physics (Mollison, 1995).

Epidemics have been modeled using differential equations (Edelstein-Keshet, 1988; Murray, 1993). However this approach has some serious drawbacks (Ahmed and Agiza, 1998) in that it neglects the local character of the spreading process, it does not include variable susceptibility of individuals, and cannot handle the complicated boundary and initial conditions. Cellular automata (CAs) can overcome the above drawbacks and have been used by several researchers as an alternative method of modeling epidemics (Jo-

* Corresponding author. Tel.: +30-541-79548; fax: +30-541-29813.

E-mail address: ykar@demokritos.cc.duth.gr (I. Karafyllidis).

0304-3800/00/$ - see front matter
PII: S0304-3800(00)00294-5

hansen, 1996; Vlad et al., 1996, Zaharia et al., 1996; Kleczkowski et al., 1997; Rousseau et al., 1997; Ahmed and Agiza, 1998; Ahmed et al., 1998; Dos Santos, 1998; Rhodes and Anderson, 1998; Maniatty et al., 1999).

The aim of this work is to use the CA approach in order to study the effect of population movement on epidemic propagation. We have developed a two-dimensional CA model, each cells of which represents a part of the total population, which may be found in one of three states: infected, immunized and susceptible. As parts of the population move randomly in the CA lattice, the disease spreads. We have studied the effect of the two most important population movement parameters on the epidemic propagation: the distance of movement and the percentage of the population that moves. Finally, the model has been extended to include the effect of the vaccination of some parts of the population on epidemic propagation. The proposed model can serve as a basis for the development of algorithms to simulate real epidemics based on real data.

The paper is organized as follows: in Section 2, a summary of the differential equations used to model epidemic propagation is given. All the necessary background on CAs is given in Section 3. The model is described in Section 4. Based on this model, we develop an algorithm for the simulation of epidemic spreading. The algorithm is described in Section 5, and the corresponding pseudocode is given. The implementation of the algorithm in the homogeneous spreading of the epidemic is described in Section 6. The effect of the population movement and the effect of vaccination of some parts of the population on epidemic propagation are described in Section 7 and Section 8, respectively. Finally, the discussion of the results obtained in the previous sections and the conclusions drawn are presented in Section 9.

2. Differential equations for modeling epidemic spreading

Differential equation models are used to describe epidemic models (Holmes, 1997; Ahmed and Agiza, 1998), e.g. the Kermack and McKendrick (1927) SIR model, with the system of ordinary differential equations:

$$\dot{S} = -aSI, \quad \dot{I} = aSI - bI, \quad \dot{R} = bI \tag{1}$$

where S is the susceptible part, I the infected part, and R the recovered part of the population.

Here, it is assumed that the population is well mixed, an assumption which in reality is not valid. Also, it is assumed that the total population is constant, i.e. external effects, such as death, movement, imported objects etc. are neglected. The variable susceptibility of individuals is also neglected. When incubation is included, the resulting equation determining the asymptotic value of susceptibles is the complicated self-consistent transcendental equation (Jones and Sleeman, 1983):

$$S(\infty) = S(0) \exp\left(-a \int_0^{\sigma} I_0(u)du - a\sigma[S(0) - S(\infty)] \right) \tag{2}$$

where $I_0(t)$ is the number of initial infectives remaining at time t. In Section 4, we will use the cellular automata approach, which avoids these complications.

3. Cellular automata

CAs (von Neumann, 1966) are models of physical systems, where space and time are discrete and interactions are local. They have been extensively used as models for complex systems (Wolfram, 1994). CAs have also been applied to several physical problems, where local interactions are involved (Gerhard and Schuster, 1989; Gerhard et al., 1990; Weimar et al., 1992; Karafyllidis and Thanailakis, 1997, Karafyllidis, 1998). In spite of the simplicity of their structure, CAs exhibit complex dynamical behavior and can describe many physical systems and processes. A CA consists of a regular uniform n-dimensional lattice (or array), usually of infinite extent. At each site of the lattice (cell), a physical quantity takes on values. This physical quantity is the global state of the CA, and the value of this quantity at each site is its local state. Each cell is

restricted to local neighborhood interaction only and, as a result, it is incapable of immediate global communication (von Neumann, 1966). The neighborhood of a cell is taken to be the cell itself and some (or all) of the immediately adjacent cells. The states at each cell are updated simultaneously at discrete time steps, based on the states in their neighborhood at the preceding time step. The algorithm used to compute the next cell state is referred to as the CA local rule. Usually, the same local rule applies to all cells of the CA.

A CA is characterized by five properties:

1. the number of spatial dimensions (n);
2. the width of each side of the array (w). w_j is the width of the jth side of the array, where $j = 1, 2, 3, \ldots, n$;
3. the width of the neighborhood of the cell (d). d_j is the width of the neighborhood along the jth side of the array;
4. the states of the CA cells;
5. the CA rule, which is an arbitrary function F.

The state of the a cell, at time step $(t+1)$, is computed according to F. F is a function of the state of this cell at time step (t) and the states of the cells in its neighborhood at time step (t). The case of a two-dimensional CA ($n = 2$), with neighborhood width $d_1 = 3$ and $d_2 = 3$, is shown in Fig. 1. In this case the neighborhood of the (i, j) cell consists of the (i, j) cell itself and of all eight cells which are adjacent and diagonal to it.

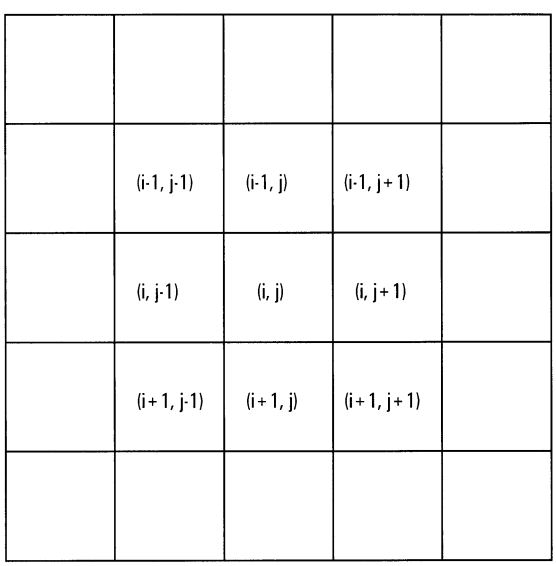

Fig. 1. The neighborhood of the (i, j) cell is formed by the (i, j) cell itself and the eight adjacent cells.

CAs have sufficient expressive dynamics to represent phenomena of arbitrary complexity and, at the same time, can be simulated exactly by digital computers because of their intrinsic discreteness, i.e. the topology of the simulated object is reproduced in the simulating device (Vichniac, 1984). Mathematical tools for simulating physics, namely PDEs, contain much more information than is usually needed, because variables may take an infinite number of values in a continuous space. Moreover, the value of a physical quantity cannot be measured at a point, but instead it is measured over a finite volume (Toffoli, 1984a). PDEs are used to compute values of physical quantities at points, whereas CAs are used to compute values of physical quantities over finite volumes (CA cells). The CA approach is consistent with the modern notion of unified space-time. In computer science, space corresponds to memory and time to processing unit. In CAs, memory (CA cell state) and processing unit (CA local rule) are inseparably related to a CA cell (Matzke, 1994; Omtzigt, 1994). Therefore, for the above reasons, CAs are an alternative to partial differential equations (Toffoli, 1984a; Omohundro, 1984) and they can easily handle complicated boundary and initial conditions, inhomogeneities and anisotropies, which are induced by epidemics. In addition, algorithms based on CAs run quickly on digital computers (Toffoli, 1984b). As models for physical systems, CAs have many limitations. They are classical systems and, therefore, they cannot represent quantum mechanical systems. CAs should not be used to simulate systems where speeds are comparable to that of light because of the anisotropy induced by the discrete space. More about modeling physics with CAs may be found in Minsky, 1982, Feynman, 1982, Zeigler, 1982 and Vichniac, 1984.

Models based on CAs lead to algorithms which are fast when implemented on serial computers because they exploit the inherent parallelism of the CA structure. These algorithms are also ap-

propriate for implementation on massively parallel computers, such as the cellular automaton machine (CAM) (Toffoli, 1984b; Wilding et al., 1991).

4. Description of the model

The population over which the epidemic propagation will be modeled is assumed to exist in a two dimensional space. Furthermore, it is assumed that the population distribution is homogenous. The two dimensional space is divided into a matrix of identical square cells, with side length a and it is represented by a CA. Each CA cell includes a number of individuals living there. The number of spatial dimensions of the CA array is $n=2$. The widths of the two sides of the CA array are taken to be equal, i.e. $w_1=w_2$. The size of the array (i.e. the values of $w_{1,2}$) is defined by the user of the model and it is a compromise between accuracy and computation time. A large array size results in a large number of CA cells with small side length a, thus, increasing the model accuracy, but it also results in large computations times. The width of the neighborhood of a CA cell is taken to be $=3$ in both array sides, i.e. $d_1=d_2=3$. This CA cell neighborhood is shown in Fig. 1.

The state $C^t_{i,j}$ of the (i,j) CA cell at time t is:

$$C^i_{i,j}=\{P^i_{i,j}, \mathrm{INF}^t_{i,j}, \mathrm{IMF}^t_{i,j}\} \tag{3}$$

where $\mathrm{INF}^t_{i,j}$ is a flag called the 'infectious flag'. The value of this flag indicates whether some of the individuals located in the (i,j) cell are infected by the disease at time t. If $\mathrm{INF}^t_{i,j}=1$, then the (i,j) cell belongs to the set of infected cells of the population, because some of the individuals of this cell are infected by the epidemic disease, whereas if $\mathrm{INF}^t_{i,j}=0$, then none of the individuals located in the (i,j) cell is infected by the epidemic. If $\mathrm{INF}^t_{i,j}=1$, then $P^t_{i,j}$ is the fraction of the number of individuals in the (i,j) cell infected by the disease, at time t:

$$P^t_{i,j}=\frac{S^t_{i,j}}{T^t_{i,j}} \tag{4}$$

where $S^t_{i,j}$ is the infected part of the population and $T^t_{i,j}$ is the total population in the (i,j) cell.

$P^t_{i,j}$ may take any value between 0 and 1, but, in order to keep the number of states of the CA finite, $P^t_{i,j}$ is made to take 11 discrete values:

$$\begin{aligned}
&\text{If } 0.0<P^t_{i,j}<0.1, \quad \text{then } P^t_{i,j}=0.1\\
&\text{If } 0.1\le P^t_{i,j}<0.2, \quad \text{then } P^t_{i,j}=0.2\\
&\cdots\cdots\cdots\cdots\cdots\cdots\\
&\text{If } 0.9\le P^t_{i,j}\le 1.0, \quad \text{then } P^t_{i,j}=1.0
\end{aligned} \tag{5}$$

Obviously, if $\mathrm{INF}^t_{i,j}=0$, then $P^t_{i,j}=0$.

The time duration of the disease is user-defined and it can be assumed to be equal to t_{in}. After that time the population has recovered from the disease and has acquired a temporal immunity to this disease. After t_{in} time steps, the flag $\mathrm{INF}^t_{i,j}$ will change its value from 1 to 0. At this time, the flag $\mathrm{IMF}^t_{i,j}$ will also change its value from 0 to 1. $\mathrm{IMF}^t_{i,j}$ is called the 'immune flag' and indicates whether the population located in the (i,j) cell is immune to the disease or not. The immune population loses its immunity after time t_{im}, it becomes susceptible to the disease again and the value of the flag $\mathrm{IMF}^t_{i,j}$ becomes equal to 0. The time duration t_{im} is also user-defined.

Recapitulating, the CA cells may be found in one of the following three general states:

If $\mathrm{INF}^t_{i,j}=0$, and $\mathrm{IMF}^t_{i,j}=0$, then the population in the (i,j) cell is susceptible to the disease.

If $\mathrm{INF}^t_{i,j}=1$, $\mathrm{IMF}^t_{i,j}=0$, and $0<P^t_{i,j}\le 1$, then the population in the (i,j) cell is infected.

If $\mathrm{INF}^t_{i,j}=0$, and $\mathrm{IMF}^t_{i,j}=1$, then the population in the (i,j) cell is immune to the disease.

It is clear that the value of $P^t_{i,j}$ is considered only in the case where the population is infected. In the other two cases, its value is 0. For example, the state of a cell with 55% of its population infected is $C^t_{i,j}=\{0.55, 1, 0\}$.

Each CA cell starts as susceptible and becomes infected if some CA cell in its neighborhood is infected. It remains infected for time t_{in} and then it becomes immune. It remains immune for time t_{im} and then it becomes susceptible again. The transition from the infected state to the immune state takes place after time t_{in}. The transition from the immune state to the susceptible state takes place after time t_{im}. The transition from the susceptible state to the infected state is done according to:

Pseudocode	Comments
1). Start	
2). Set t=1	
3). Read the properties of the initial population	/* This is the initial state of the CA */
4). Set t=t+1	/* Take a time step */
5). Determine which CA cells include individuals that are infected, and which CA cells include individuals that are not infected, i.e. check the $INF^{t}_{i,j}$ and the $IMF^{t}_{i,j}$	
6). If $IMF^{t}_{i,j}$=1	
go to 8	
else	
go to 7	
7). Compute the percentage of the individuals of each CA cell being infected, using the CA local rule	/* Use equation (6) */
8). If t is less than T_e then	/* T_e is the user defined duration of the epidemic's process */
go to 4	
else	
produce output	/* Schematic representation of the epidemic propagation */
9). Stop	

Fig. 2. The pseudocode of the algorithm.

$$P^{t+1}_{i,j} = P^{t}_{i,j+k}(P^{t}_{i-1,j}, P^{t}_{i,j-1}, P^{t}_{i,j+1}, P^{t}_{i+1,j}) + l(P^{t}_{i-1,j-1}, P^{t}_{t-1,j+1}, P^{t}_{i+1,j-1}, P^{t}_{i+1,j+1}) \quad (6)$$

The state $P^{t+1}_{i,j}$, of the (i, j) cell at the next time step $t+1$, is affected by the states of all eight cells in its neighborhood at the present time step t, and by its own state at the present time step t. The CA local rule comprises the transitions between the states, as described above and Eq. (6). In Eq. (6), the adjacent nearest neighbors of the (i, j) cell, i.e. the neighbors that have a common side with the (i, j) cell and the diagonal adjacent neighbors are grouped, respectively, together. The effect of the adjacent nearest neighbors is multiplied by k, whereas the effect of the diagonal adjacent neighbors is multiplied by l. It is expected that the (i, j) cell will be infected more quickly, if it has an infected adjacent nearest neighbor than if it has an infected diagonal adjacent neighbor, because of the more extensive contact between populations. Therefore, it is always $k > l$.

5. The algorithm

An algorithm for the simulation of the epidemic spreading, based on the model described in Section 4, has been developed in the present research work. Fig. 2 shows the pseudocode of this algorithm. In the beginning, the algorithm reads the initial state of the CA cell. The number of cells is defined by the user and it is a compromise between accuracy and computation time. In the next time step, the flags of the CA cells are considered to determine which cells include individuals infected or immune. After that, the algorithm calculates the percentage of the infected individuals in

all CA cells, using Eq. (6). Subsequently, the termination condition is applied. This condition is usually a number of time steps T_e defined by the user. If the number of time steps taken is less than T_e, the algorithm continues by taking another time step. If the number of time steps taken is equal to or greater than T_e, the algorithm terminates.

6. Homogeneous process of epidemic propagation

The spreading of the epidemic is homogeneous if the initial properties of the population of CA cells are the same for all cells. Consider that the epidemic process starts at a point in the center of the two dimensional space, where the population exists. In this case, the epidemic fronts should be circular and this was the first test to the proposed model. Successive epidemic fronts, almost perfect circles, have been obtained as shown in Fig. 3. The algorithm, in this particular case, was applied to a matrix of 100×100 cells and it was found that, for the model to produce circular epidemic fronts, the values of the parameters k and l of the local CA rule should be 0.44 and 0.04, respectively. In Fig. 3, the central CA cell is assumed to be infected and that it spreads the disease to its neighborhood, the epidemic process finishing after $T_e = 40$ time steps. The infection and immune times are chosen to be $t_{in} = 5$ and $t_{im} = 10$. As shown in Fig. 3, the population of the CA cells is divided into four regions. In region (1) the CA cells include susceptible individuals. The individuals in this region have previously been infected, immunized, and become susceptible again. The CA cells, which are found in region (2), include individuals who have been infected in the past and are now immune. In region (3), the CA cells include individuals who are currently infected. Finally, in region (4) the CA cells include individuals who have not yet been in contact with the epidemic disease and, thus, they are not infected.

Fig. 4a shows the case where the central CA cell of the population, after it had completed the epidemic process (infected–immunized–susceptible), is infected again by the same disease and the cycle of the epidemic is resumed. This results in concentric circles expressing the resumption of the epidemic from the center of the population. The parameters of the algorithm remain the same as in the case of Fig. 3, the main difference focusing on

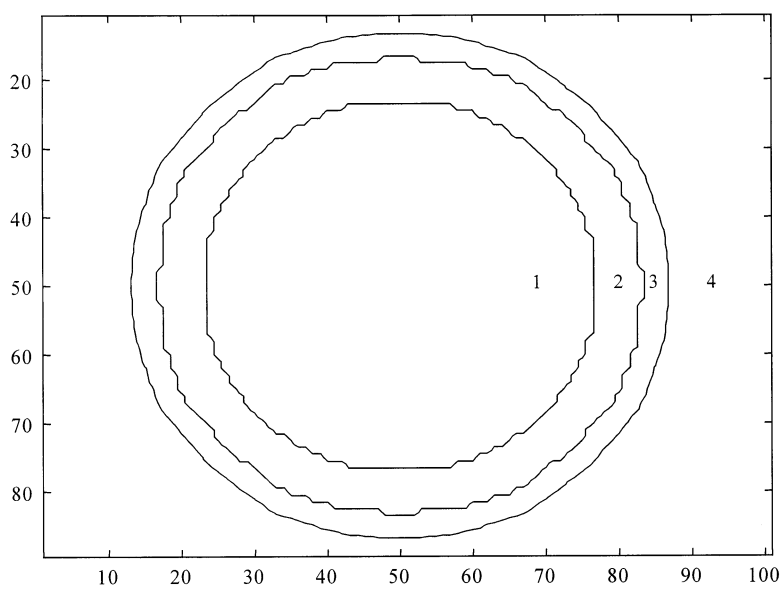

Fig. 3. Circular epidemic fronts. The epidemic starts at the center of the circular fronts. The population of CA cells is divided into four regions (1, susceptible; 2, immune; 3, infected; 4, susceptible). (The distance units in both axes are arbitrary).

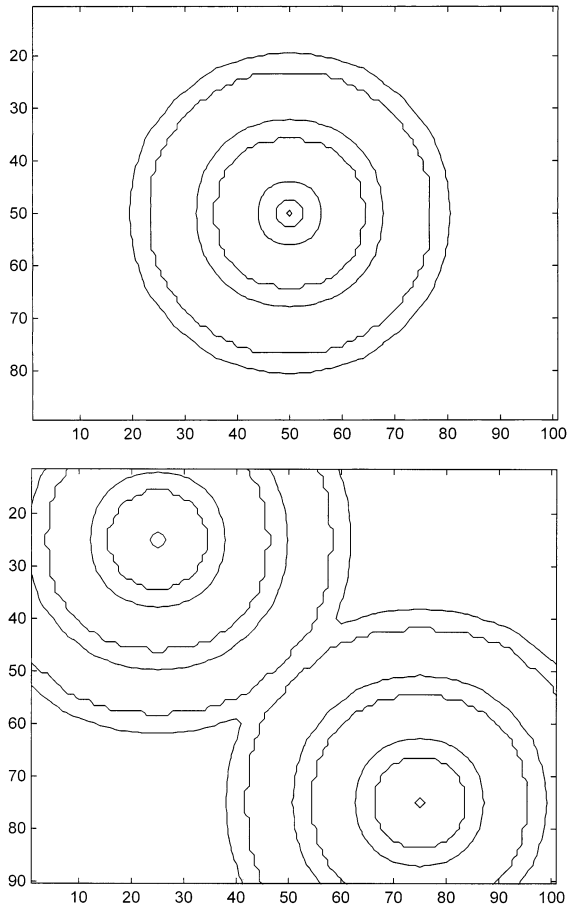

Fig. 4. Circular epidemic fronts in the case where the central CA cell of the population, after it had completed the epidemic process, is infected again by the same disease, and the cycle of the epidemic is resumed. (b) Circular epidemic fronts, almost perfect circles, in the case where two CA cells, after they had completed the epidemic process, are infected again, and the cycle of the epidemic is resumed. (The distance units in both axes are arbitrary).

the resumption of the epidemic in the center of the matrix, which creates epidemic circles with period $T = t_{in} + t_{im}$. It should be mentioned that the region of the CA cells that includes immune individuals is not represented in Fig. 3 for reasons of simplicity. The case of two CA cells being centers of epidemic spreading is shown in Fig. 4b. There is one cell on the upper left corner and one on the lower right corner of the matrix creating epidemic circles with period $T = t_{in} + t_{im}$ and the two epidemic fronts intersect after a few time steps. As in Fig. 4a, the individuals of the two cells, after completing the epidemic process, are getting infected again and a new epidemic cycle begins.

7. The effect of population movement

One of the most important factors for the propagation of an epidemic disease in a population is the movement of individuals. This results in an increment of the individuals getting infected and in the enlargement of the overall percentage of the infected population. The effect of the population movement is included in the algorithm developed in this work. The distance of movement and the number of individuals who are going to move are the two most important parameters which are taken into consideration. Fig. 5a shows the epidemic front resulting from the movement of individuals. It should be mentioned that in Fig. 5, the infection and immune times were chosen to be $t_{in} = 15$ and $t_{im} = 30$, respectively, whereas the movement of individuals was taking place after $t_m = 30$ time steps from the beginning of the epidemic process. In Fig. 5a, the epidemic front for $T_e = 40$ time steps is shown and, as in Fig. 3, the central CA cell was assumed to be infectious and that it spread the epidemic to its neighborhood only once. The percentage of the population that was going to move was taken to be $= 10\%$, while the maximum distance of movement was taken to be: max_distance equals five array cells. The cells involved in the population movement were chosen with the help of a pseudorandom number generator (Knuth, 1981), which provides the new locations, in every possible direction, with a maximum distance of five array cells. The distance of the movement could be randomly different for each of the chosen cells and it also results from a pseudorandom number generator (Knuth, 1981), with the single limitation that this distance cannot be greater than the maximum distance. To obtain a greater variability, the possible direction of population movement is decided randomly, i.e. the individuals of the chosen CA cell (i, j), could move to the CA cell $(i \pm x, j \pm x)$, where $0 \leq x \leq 5$. In Fig. 5b, the epidemic front is just as before,

but this time the percentage of the population, which is about to move has increased to 20%. The rest of the parameters, T_e, t_m, t_{im}, t_{in} and max_distance, were exactly the same as in Fig. 5a. Similarly, Fig. 5c,d show the epidemic fronts for population movements of 30 and 40%, respectively, the other parameters of the algorithm again remaining the same.

If the maximum distance is increased, the propagation of the epidemic will be faster. In Fig. 6a, the percentage of the population that moves was taken to be $=10\%$, while the maximum distance of movement was taken to be equal to: max_distance equals ten array cells. Also, the infection and the immune times were chosen to be $t_{in}=15$ and $t_{im}=30$, respectively, whereas the movement of the individuals starts after $t_m=30$ time steps from the beginning of the epidemic process. Finally, the epidemic front was depicted for $T_e=40$ time steps. The only difference between Fig. 5a and Fig. 6a is located on the value of max_distance, which was doubled in the latter case. In Fig. 6b–d, the parameters of the algorithm remain the same, except for the percentages of the population that move. These are increasing by 10%. Thus, in Fig. 6b, the percentage of the population that moves has increased to 20%, in Fig. 6c that percentage is $=30\%$ and, finally, in Fig. 6d, the percentage is 40%. The differences between Fig. 5 and Fig. 6 are obvious. When the

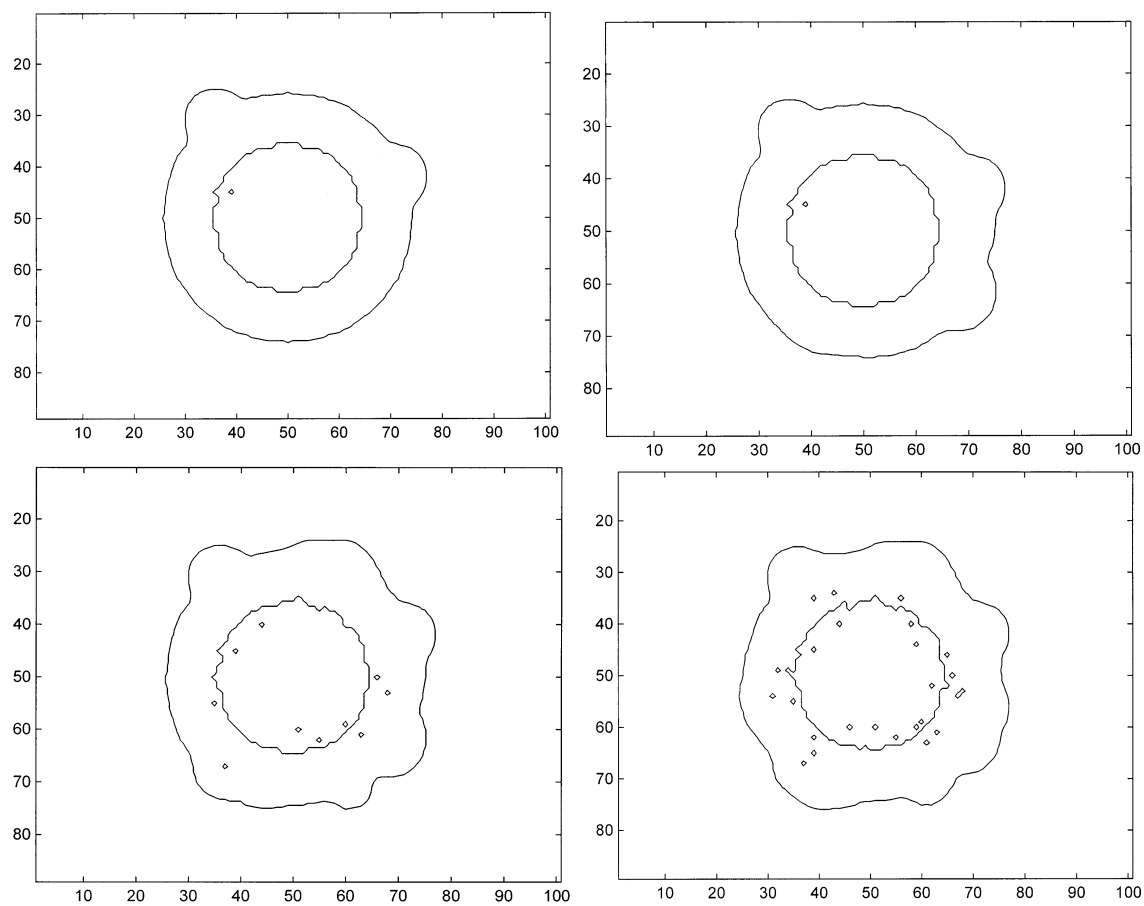

Fig. 5. Circular epidemic fronts in the case of random population movement, with a maximum distance equal to five array cells and a percentage of moving population: (a) 10%, (b) 20%, (c) 30% and (d) 40% of the total population. (The distance units in both axes are arbitrary).

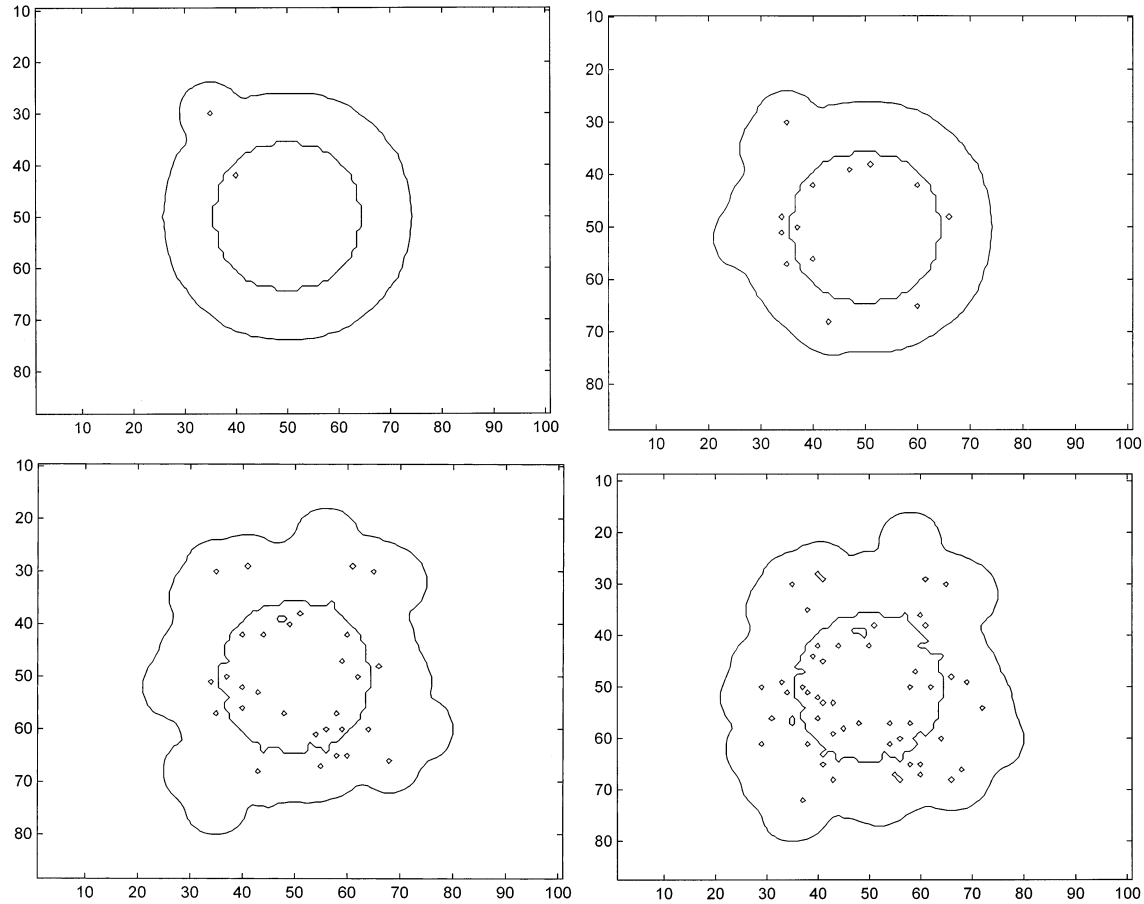

Fig. 6. Circular epidemic fronts in the case of random population movement, with a maximum distance equal to ten array cells and a percentage of moving population: (a) 10%, (b) 20%, (c) 30% and (d) 40% of the total population. The fronts of Fig. 5(a) and Fig. 6(a), Fig. 5(b) and Fig. 6(b), Fig. 5(c) and Fig. 6(c), and Fig. 5(d) and Fig. 6(d) correspond to the same set of parameters. The only difference is the maximum distance of population movement. (The distance units in both axes are arbitrary).

percentage of the moving population is increased, the epidemic fronts lose their symmetry, and the spreading of the epidemic disease is accelerated.

Finally, the case of increasing even more the value of max_distance is considered and the results obtained are presented in the Fig. 7a–d. The value of max_distance is now 15 and for Fig. 7a, the percentage of the moving population is 10%, while the rest of the parameters remain equal to those corresponding to Fig. 5 and Fig. 6. Similarly, Fig. 7b–d depict the epidemic fronts, which have resulted from the population movement in percentages of 20, 30 and 40%, respectively. It should be noticed that as the max_distance and the percentage of moving population are increased, the epidemic fronts lose their circular shape and the epidemic spreading is accelerated.

The influence of the differences in the percentages of moving populations on the epidemic spreading is better expressed in Fig. 8a. In Fig. 8, there are four lines indicating the normalized area covered by the epidemic disease after the movement of population at time step 30. The line, numbered 1, represents the normalized area covered by the epidemic disease in the case where the moving population is 10% of the whole population and the maximum distance of this movement is equal to five array cells, as it was shown in

Fig. 5a. The line, numbered 2, corresponds to Fig. 5b, where the percentage of the moving population was 20% and the maximum distance of this movement was again equal to five array cells. Lines, numbered 3 and 4, resulted from Fig. 5c,d respectively, represent the normalized area covered by the epidemic disease in the cases of 30 and 40% of moving population, with the maximum distance being equal to five array cells. In Fig. 8b, there are also four lines representing the normalized area covered by the epidemic, but this time, the maximum distance is equal to ten array cells. Again, line 1 corresponds to Fig. 6a, line 2 to Fig. 6b, line 3 to Fig. 6c, and line 4 to Fig. 6d. Comparing with Fig. 8a, it can be easily seen that increasing the maximum distance of population movement leads to an increment in the normalized area covered by the epidemic disease. Furthermore, the results with different percentages of moving population are better seen in Fig. 8b, as lines 3 and 4 deviate from lines 1 and 2 to a larger extent than in the case of Fig. 8a. Finally, in Fig. 8c (curves 1–4) is shown the normalized area covered by the epidemic in the cases corresponding to Fig. 7a–d, respectively. As mentioned before, in the cases of Fig. 7, the maximum distance of possible population movement was changed to 15 array cells, while none of the other parameters

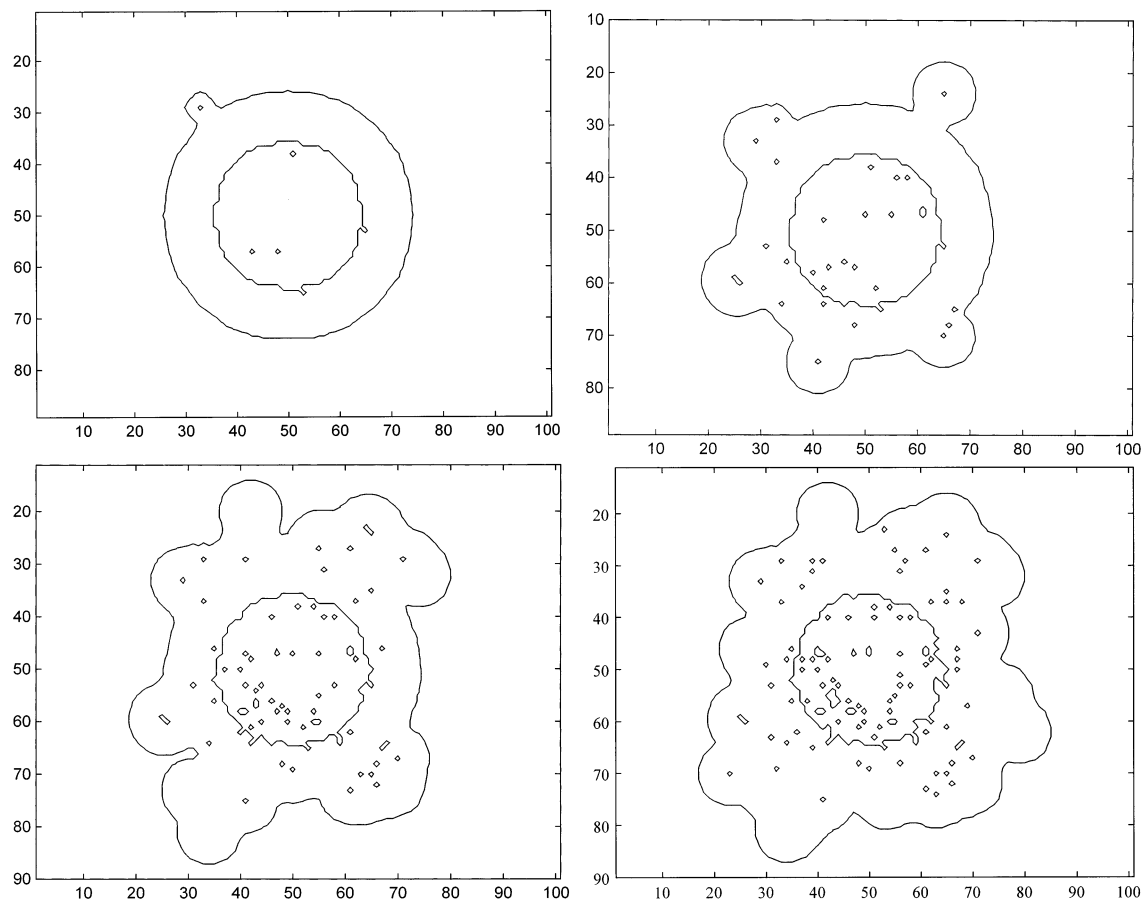

Fig. 7. Circular epidemic fronts in the case of random population movement, with a maximum distance equal to 15 array cells and a percentage of moving population: (a) 10%, (b) 20%, (c) 30% and (d) 40% of the total population. The fronts of Fig. 5(a) and Fig. 7(a), Fig. 5(b) and Fig. 7(b), Fig. 5(c) and Fig. 7(c), and Fig. 5(d) and Fig. 7(d) correspond to the same set of parameters. The only difference is the maximum distance of population movement. (The distance units in both axes are arbitrary).

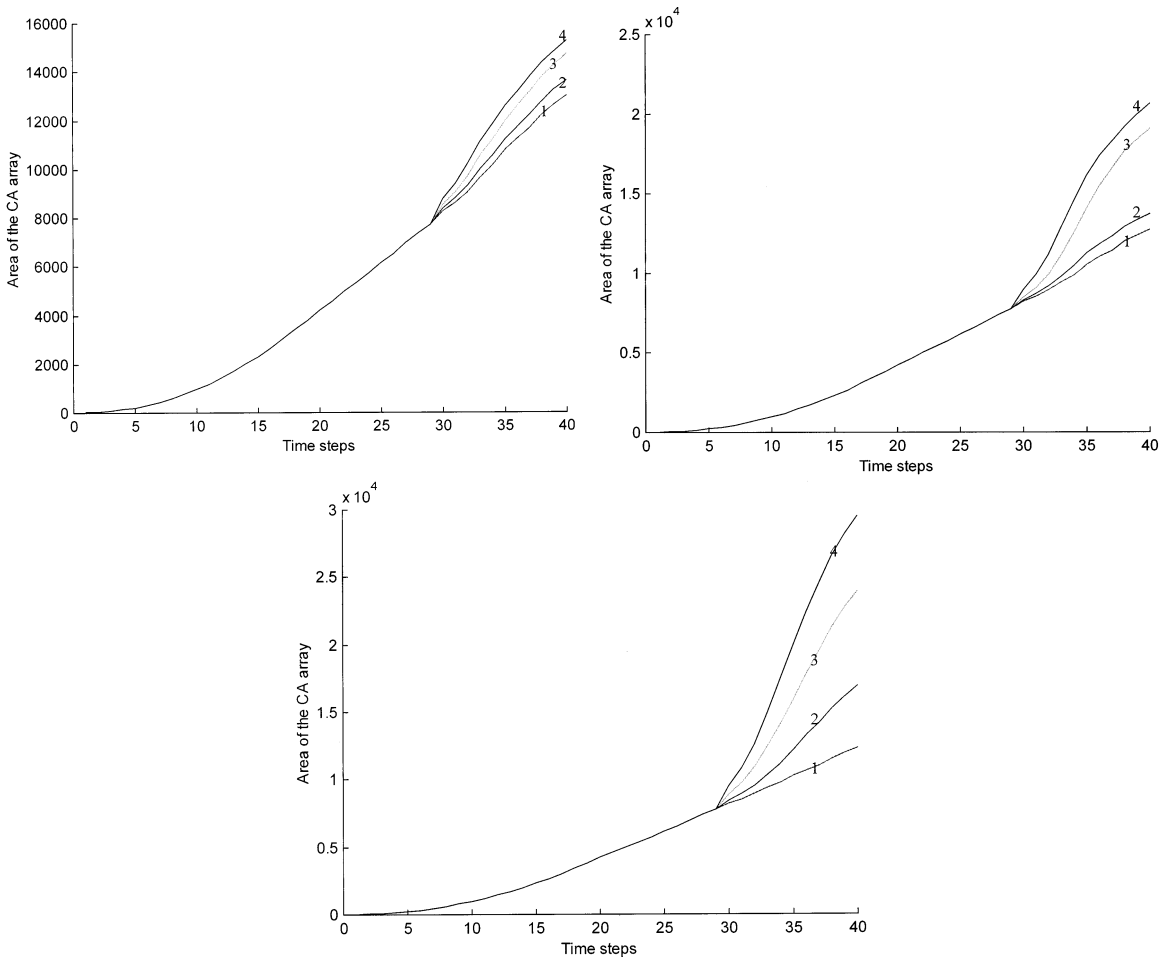

Fig. 8. The normalized area covered by the epidemic disease as a function of time, in the case of random population movement with maximum distance equal to five array cells and a percentage of moving population: 10% (curve 1), 20% (curve 2), 30% (curve 3) and 40% (curve 4) of the total population. (b) The normalized area covered by the epidemic disease as a function of time in the case of random population movement with maximum distance equal to ten array cells and a percentage of moving population: 10% (curve 1), 20% (curve 2), 30% (curve 3) and 40% (curve 4) of the total population. (c) The normalized area covered by the epidemic as a function of time in the case of random population movement with maximum distance equal to 15 array cells and a percentage of moving population: 10% (curve 1), 20% (curve 2), 30% (curve 3) and 40% (curve 4) of the total population.

of the algorithm, applied to the cases of Fig. 5 and Fig. 6, had been changed for the set of Fig. 7. As before in Fig. 8a,b, in Fig. 8c there are four lines (numbered 1–4) expressing the normalized area covered by the epidemic in the cases of different percentages of moving population, equal to 10, 20, 30 and 40%, respectively. In comparison with Fig. 8a,b, Fig. 8c shows more clearly the divergence of the four lines numbered 1–4.

8. The effect of vaccination of the population

The purpose of prophylactic vaccination is to reduce morbidity and mortality in a population. The effect of population vaccination reduces the epidemic spreading, which is falling progressively. To simulate the effect of vaccination, using the algorithm of this work, we assume that a small part of the initial population is vaccinated, as it is

shown in Fig. 9a. To extend the variability of the effect of vaccination, the location and size of the vaccinated population was chosen randomly. In Fig. 9b, the epidemic front has just reached the part of vaccinated population and is going to spread beyond it at subsequent time steps. The infection and the immune times were chosen to be $t_{in} = 15$ and $t_{im} = 30$, respectively, just as before. In Fig. 9c, it is shown that the vaccinated population is not infected by the epidemic, although the epidemic has infected all other cells in the neighborhood of the vaccinated population. Moreover, as shown in Fig. 9d, the vaccinated population helps in the reduction of the epidemic spreading near the neighborhood of vaccination, distorting the roundness of the circular epidemic front and causing a small irregularity in the development of the epidemic. The effect of population vaccination on the epidemic spreading depends, normally, on the percentage of the vaccinated population. In the case of a small percentage of the population being vaccinated, considered in this paper, the vaccination does not change dramatically the spreading of the epidemic, as shown in Fig. 9e, where the epidemic front has almost regained its normal shape. However, it does give a good picture of how the vaccination effect is simulated by the algorithm developed in this work.

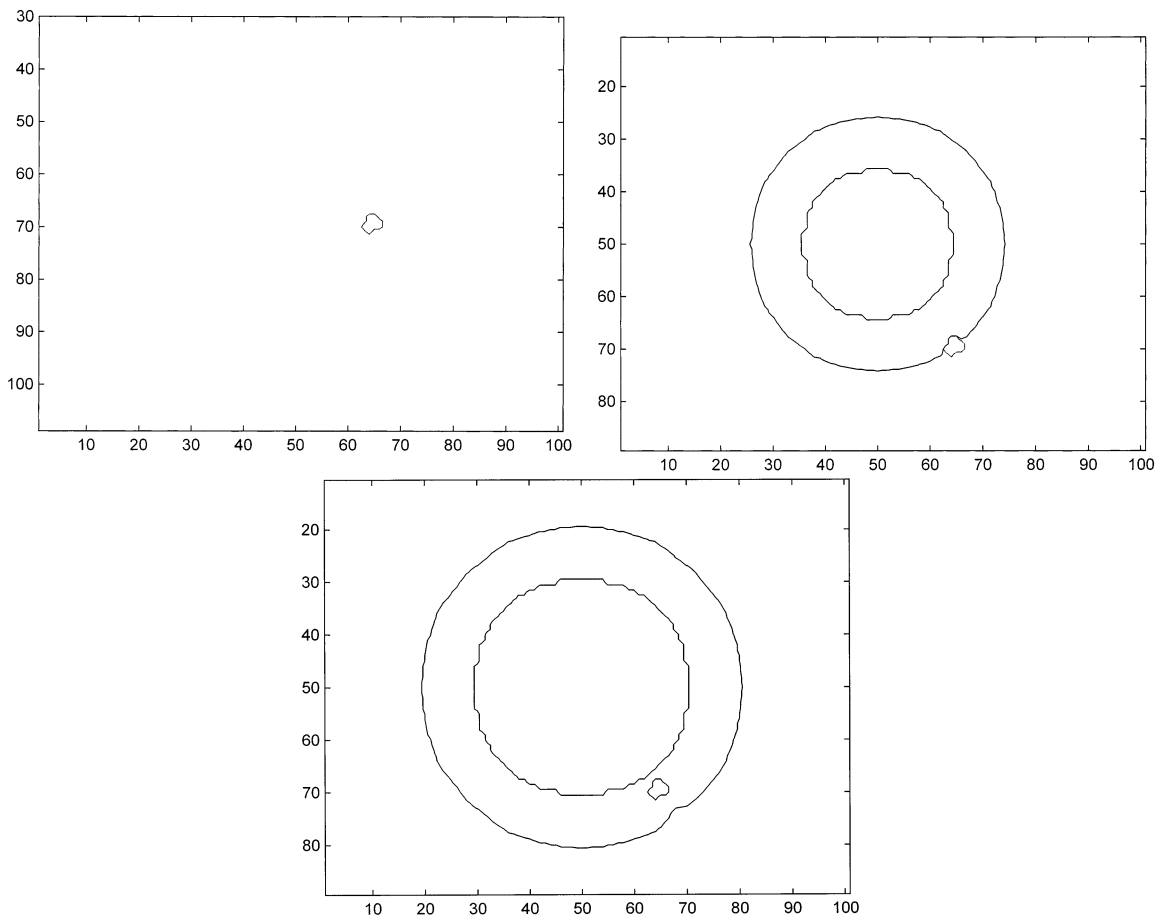

Fig. 9. A small part of the initial population is assumed to be vaccinated. (b) The epidemic front has just reached the part of vaccinated population, and it is going to spread beyond it at subsequent time steps. (c) The epidemic has infected all the cells in the neighborhood of the vaccinated population but not the vaccinated population. (d) The vaccinated population helps into the reduction of epidemic spreading near the neighborhood of vaccination, distorting the roundness of the circular epidemic front and causing a small irregularity in the development of the epidemic. (e) The epidemic front has almost regained its normal shape.

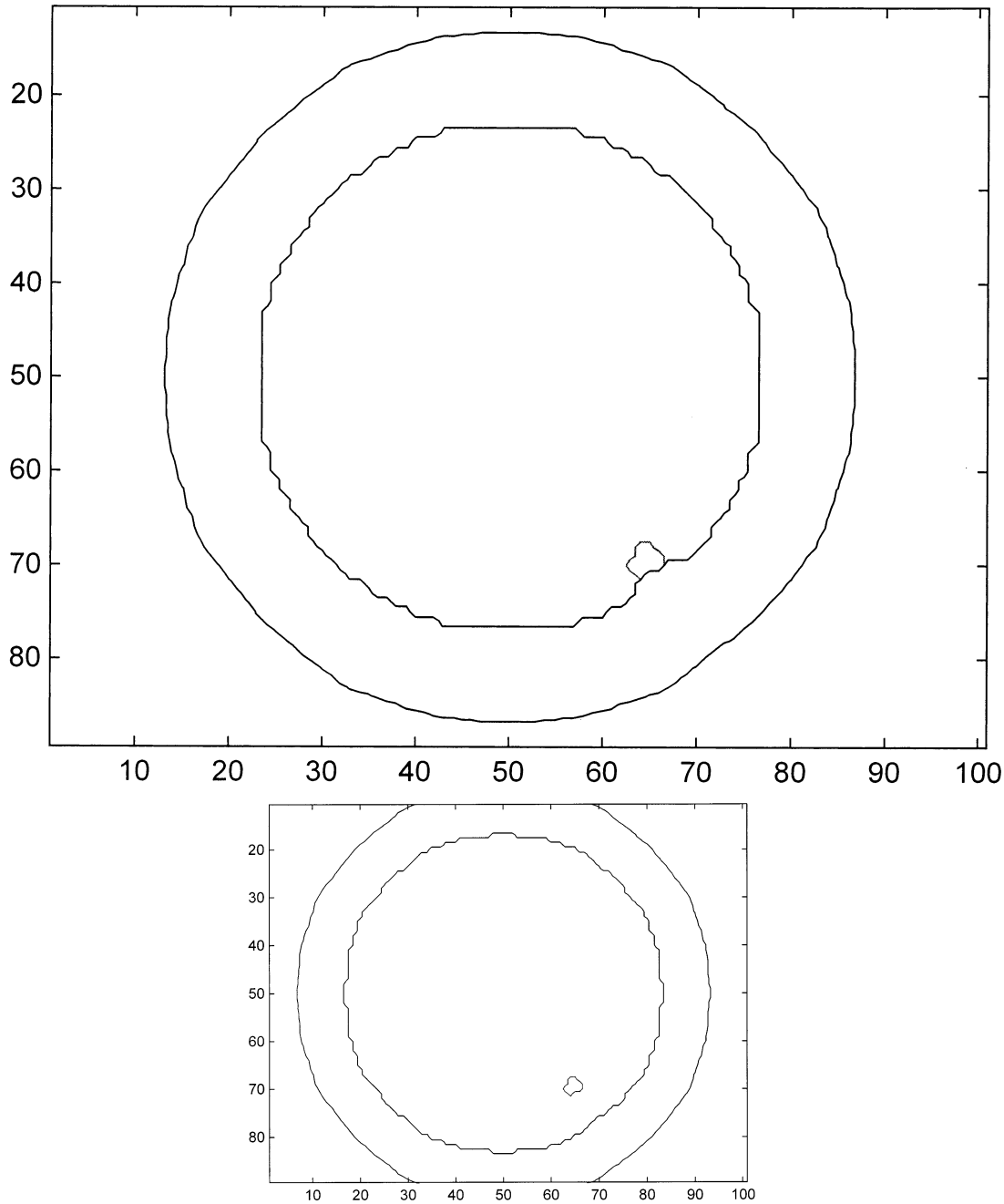

Fig. 9. (*Continued*)

9. Discussion and conclusions

In the case of homogeneous epidemic spreading, where the initial properties of the population of cells of the aforementioned CA algorithm, are the same for all cells, our algorithm managed to

produce successive circular epidemic fronts, as it was expected by theory. The simplicity of implementation of the above CA model results from the lack of complicated timeless computations derived from complex mathematical formulas, in order to produce circular fronts (Delorme et al., 1999). Furthermore, this CA algorithm has succeeded in handling both the resumption of the epidemic in the center of the matrix, which creates epidemic circles and the resumption of the epidemic in the two corners of the matrix. The effect of the population movement when implemented in the algorithm results in an increment of the individuals getting infected and in the enlargement of the overall percentage of the infected population. The distance of movement and the number of individuals who are going to move are the two most important parameters, which are taken into consideration by our algorithm. The increment of the aforementioned parameters resulted in our algorithm in the same way, as it is theoretical assigned, i.e. when the percentage of the moving population is increased, or the maximum distance of population movement is increased, the epidemic fronts lose their symmetry (i.e. their circular shape) and the spreading of the epidemic disease is accelerated. It is more than obvious that if both the parameters are increased simultaneously the epidemic process accelerates in the maximum degree. On the contrary, the effect of population vaccination reduces the epidemic spreading, which is falling progressively, because it reduces morbidity and mortality in a population. The vaccinated population helps in the reduction of the epidemic spreading near the neighborhood of vaccination, distorting the roundness of the circular epidemic front and causing a small irregularity in the development of the epidemic. The effect of population vaccination on the epidemic spreading depends, normally, on the percentage of the vaccinated population. In the case of a great percentage of the population being vaccinated, the vaccination does changes dramatically the spreading of the epidemic.

In conclusion, a cellular automaton (CA) model for epidemic propagation, including the effects of population movement and population vaccination, has been presented. An algorithm based on this model has been developed and used to determine the effect of movement of individuals, in a hypothetical homogeneous population, on the epidemic propagation. The model and algorithm were extended to include the vaccination effect. It has been shown in this work that cellular automata are suitable for modeling successfully such a complicated non-linear problem, whereas is practically impossible to use differential equations because of the complexity of the problem. Furthermore, because of the inherent parallelism of CAs, algorithms based on the proposed model can potentially run on a parallel computer. The proposed model can serve as a basis for the development of algorithms to simulate real epidemics based on real data.

References

Ahmed, E., Agiza, H.N., 1998. On modeling epidemics. Including latency, incubation and variable susceptibility. Physica A 253, 347–352.

Ahmed, E., Agiza, H.N., Hassan, S.Z., 1998. On modeling hepatitis B transmission using cellular automata. J. Stat. Phys. 92, 707–712.

Delorme, M., Mazoyer, J., Tougne, L., 1999. Discrete parabolas and circles on 2d cellular automata. Theoret. Comput. Sci. 218, 347–417.

Dos Santos, Z., 1998. Using cellular automata to learn about the immune system. Int. J. Mod. Phys. C 9, 793–799.

Edelstein-Keshet, L., 1988. Mathematical Models in Biology. Randon House, New York, NY.

Feynman, R.P., 1982. Simulating physics with computers. Int. J. Theor. Phys. 21, 467–488.

Gerhard, M., Schuster, H., 1989. A cellular automaton describing the formation of spatially ordered structures in chemical systems. Physica D 36, 209–221.

Gerhard, M., Schuster, H., Tyson, J.J., 1990. A cellular automaton model of excitable media. Physica D 46, 392–415.

Holmes, E.E., 1997. Basic epidemiological concepts in a spatial context. In: Tilman, D., Kareiva, P. (Eds.), Spatial Ecology. Princeton University Press, NJ, pp. 111–136.

Johansen, A., 1996. A simple model of recurrent epidemics. J. Theor. Biol. 178, 45–51.

Jones, P.S., Sleeman, P.D., 1983. Differential Equations and Mathematical Biology. Allen and Unwin, London, UK.

Karafyllidis, I., 1998. A model for the influence of the greenhouse effect on insect and microorganism geographical distribution and population dynamics. Biosystems 45, 1–10.

Karafyllidis, I., Thanailakis, A., 1997. A model for predicting forest fire using cellular automata. Ecol. Model. 99, 87–97.

Kermack, W.O., McKendrick, A.G., 1927. A contribution to the mathematical theory of epidemics. Proc. R. Soc. A115, 700–721.

Kleczkowski, A., Gilligan, C.A., Bailey, D.J., 1997. Scaling and spatial dynamics in plant–pathogen systems: From individuals to populations. Proc. R. Soc. B264, 979–984.

Knuth, D., 1981. Seminumerical Algorithms. Addison Wesley, Reading, MA.

Maniatty, W., Szymanski, B., Caraco, T., 1999. High-performance computing tools for modeling evolution in epidemics. In: Proceedings of the Thirty-second Annual Hawaii International Conference on System Sciences, IEEE Computer Society Press, Los Alamitos, CA, 10 pp.

Matzke, D.J., 1994. Impact of locality and dimensionality limits on architectural trends. In: Proceedings of the Workshop on Physics and Computation, PhysComp'94, IEEE Computer Society Press, Los Alamitos, CA, pp. 30–35.

Minsky, M., 1982. Cellular vacuum. Int. J. Theor. Phys. 21, 537–551.

Mollison, D., 1995. Epidemic Models. Cambridge University Press, Cambridge, UK.

Murray, J.D., 1993. Mathematical Biology. Springer-Verlag, Heidelberg.

von Neumann, J., 1966. Theory of Self-Reproducing Automata. University of Illinois, Urbana, IL.

Omohundro, S., 1984. Modeling cellular automata with partial differential equations. Physica D 10, 128–134.

Omtzigt, E.T.L. Computational spacetimes. In: Proceedings of the Workshop on Physics and Computation, PhysComp'94, IEEE Computer Society Press, Los Alamitos, CA, 1994, pp. 239–245.

Rhodes, C.J., Anderson, R.M., 1998. Forest-fire as a model for the dynamics of disease epidemics. J. Franklin Inst. 335B, 199–211.

Rousseau, G., Giorgini, B., Livi, R., Chate, H., 1997. Dynamical phases in a cellular automaton model for epidemic propagation. Physica D 103, 554–563.

Toffoli, T., 1984a. Cellular automata as an alternative to (rather an approximation of) differential equations in modeling physics. Physica D 10, 117–127.

Toffoli, T., 1984b. CAM: a high-performance cellular automaton-machine. Physica D 10, 195–204.

Vichniac, G.Y., 1984. Simulating physics with cellular automata. Physica D 10, 96–116.

Vlad, M.O., Schonfisch, B., Lacoursiere, C., 1996. Statistical-mechanical analogies for space-dependent epidemics. Physica A 229, 365–401.

Weimar, J.R., Tyson, J.J., Watson, L.T., 1992. Diffusion and wave propagation in cellular automaton models of excitable media. Physica D 55, 309–327.

Wilding, N.B., Trew, A.S., Hawick, K.A., Pawely, G.S., 1991. Scientific modeling with massively parallel SIMD computers. Proc. IEEE 79, 574–585.

Wolfram, S., 1994. Cellular Automata and Complexity. Addison-Wesley, Reading, MA.

Zaharia, C.N., Cristea, A., Simionescu, I., 1996. The simultaneous utilisation of many techniques of the artificial intelligence in epidemics modelling. In: Bruzzone, A.G., Kerckhoffs, Chent, E.J.H. (Eds.), Proceedings of the Eighth European Simulation Symposium Simulation in Industry, vol. 2. SCS, Belgium, pp. 142–146.

Zeigler, B.P., 1982. Discrete event models for cell space simulation. Int. J. Theor. Phys. 21, 573–588.